CASE 1: A REDUCED-ORDER MODEL FOR ZERO-MASS SYNTHETIC JET ACTUATORS

Nail. K. Yamaleev[1], Mark H. Carpenter[2], and Veer S. Vatsa[2]

[1]*Department of Mathematics, North Carolina A&T State University, Greensboro, NC 27410*
[2]*Computational Modelling & Simulation Branch, NASA Langley Research Center, Hampton, VA 23681*

Introduction

Accurate details of the general performance of fluid actuators is desirable over a range of flow conditions, within some predetermined error tolerance. Designers typically model actuators with different levels of fidelity depending on the acceptable level of error in each circumstance. Crude properties of the actuator (e.g., peak mass rate and frequency) may be sufficient for some designs, while detailed information is needed for other applications (e.g., multiple actuator interactions).

This work attempts to address two primary objectives. The first objective is to develop a systematic methodology for approximating realistic 3-D fluid actuators, using quasi-1-D reduced-order models. Near full fidelity can be achieved with this approach at a fraction of the cost of full simulation and only a modest increase in cost relative to most actuator models used today. The second objective, which is a direct consequence of the first, is to determine the approximate magnitude of errors committed by actuator model approximations of various fidelities. This objective attempts to identify which model (ranging from simple orifice exit boundary conditions to full numerical simulations of the actuator) is appropriate for a given error tolerance.

Solution Methodology

The solution methodology used for this work is described in detail elsewhere [1]. Only the general aspects of the approach will be replicated herein. The time-dependent 2-D Navier-Stokes equations are used to describe the unsteady compressible flow generated by a synthetic jet actuator. No turbulence model is used in these simulations. The governing equations in curvilinear coordinates (ξ, η) are written in conservation law form. All the length scales and dependent variables have been nondimensionalized by the orifice width d and the corresponding reference values, respectively, except for p which has been normalized by $\rho_\infty u_\infty^2$, where u_∞ has been chosen to be one tenth of the speed of sound. The viscosity coefficient μ is assumed to be constant, and the equation of state for a perfect gas is used to relate pressure to the conservation variables.

The governing equations are closed with the following boundary conditions. A no-slip boundary condition for the velocity vector and a constant wall temperature are imposed on the wall surface

$$u|_{wall} = v|_{wall} = 0, \quad T|_{wall} = T_\infty. \tag{1}$$

At the subsonic outflow boundary, a boundary condition for the pressure is imposed weakly. Characteristic conditions are applied at the upper boundary so that the vortex structures can leave the computational domain without producing perceptible spurious reflections. The unsteady flow inside the actuator cavity, generated by harmonic motion of the diaphragm, is modeled by using a new reduced-order model described in the next section.

The actuator geometry is represented as the summation of multiple subdomains, each having a high degree of smoothness. Within each subdomain, a computational grid is generated having sufficient smoothness

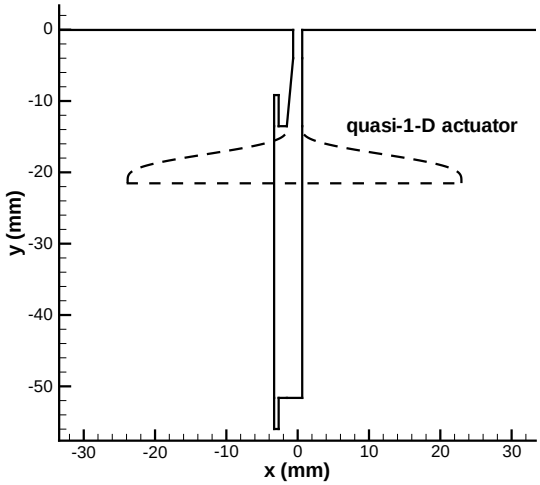

Figure 1: The 2-D and quasi-1-D geometries.

to allow solutions with three significant digits of accuracy. The connectivity at the subdomain interfaces is C_0 smooth: thus meshlines connect at interfaces but need not have smooth derivatives.

Two distinct geometries are the focus of the study. The first is a simple 2-D projection of the 3-D actuator used in Case I. The 2-D geometry of the actuator is not the centerline cut of the actual geometry, but rather is adjusted slightly so that the volume of the 2-D actuator (assuming a constant width of 1.24") is precisely that of the 3-D actuator. This was done because the volume of the actuator strongly affects the resonance characteristics of the device. The exterior portion is truncated at 100 orifice diameters. The second geometry is a subset of the first, but only includes the exterior portion of the device and the nozzle portion of the actuator. The rest of the actuator is approximated with the reduced order model, by solving the quasi-1-D Euler equations. The volume of the quasi-1-D actuator has also been chosen to be equal to the corresponding volume of the 3-D actuator. Both the 2-D and quasi-1-D geometries are shown in Fig. 1. The region where the quasi-1-D model is used is bounded by the dashed line, whereas in the rest of the domain, the 2-D Navier-Stokes equations are solved.

The grid was adjusted within the actuator and in the nearfield of the exterior to achieve two significant digits in the solution accuracy. The exterior grid was sufficient in resolution to accurately resolve the vortices near the orifice and up to ten diameters away from the orifice. Beyond that point, the mesh was expanded and the vortices were allowed to diffuse. The total number of grid points in the full 2-D and quasi-1-D simulations were 60,697 and 38,805, respectively.

A fourth-order upwind-biased linear finite difference scheme based on the local Lax-Friedrichs flux splitting is used to discretize both the 2-D Navier-Stokes equations and the quasi-1-D Euler equations. For sufficient grid smoothness within each 2-D subdomain, design order accuracy is achieved. The interfaces are connected using the penalty approach (SAT) described in detail in references [2, 3, 4, 1]. The interface penalty treatment is conservative, and maintains the underlying accuracy of the interior scheme. The SAT procedure requires co-located solution variables on both sides of the interface. The difference between the two solution values was used as a measure of spatial grid resolution. For all the simulations, the interface error was less than 0.5%.

The semi-discrete equations were explicitly integrated in time with a low-storage 4th-order Runge-Kutta scheme [5]. The simulations were all run at the maximum stable timestep. The temporal scheme has an error estimator that monitors the temporal error per timestep. The timestep error varied over the period in the range $10^{-10} - 10^{-7}$, based on the L_∞ norm of the density variable. Other solution variables had similar error norms. Each cycle required about 10^5 timesteps to complete.

Model Description

A gap exists between the 0-D models and the full 2-D/3-D models of a synthetic jet actuator. To combine the accuracy and conservation properties of the full numerical simulation methods with the efficiency of the simplified blowing/suction type boundary conditions, a new reduced-order model of a multidimensional synthetic jet actuator is proposed. In contrast to the methods available in the literature, the new approach uses a reduced-order model to approximate a 2-D or 3-D actuator. The multidimensional actuator is simulated by solving the time-dependent quasi-1-D Euler equations. The time-dependent quasi-1-D Euler equations can be written in the following conservation law form:

$$\frac{\partial \mathbf{U}}{\partial t} + \frac{\partial \mathbf{E}}{\partial y} + \mathbf{H} = 0, \tag{2}$$

$$\mathbf{U} = A \begin{bmatrix} \rho \\ \rho v \\ \rho e \end{bmatrix}, \quad \mathbf{E} = A \begin{bmatrix} \rho v \\ \rho v^2 + p \\ v(\rho e + p) \end{bmatrix}, \mathbf{H} = - \begin{bmatrix} 0 \\ p \frac{\partial A}{\partial y} \\ 0 \end{bmatrix},$$

where A is the cross-sectional area of the quasi-1-D actuator. It is assumed that A is a continuously differentiable function that is independent of time, i.e., $A = A(y)$.

To simulate the diaphragm dynamics, a time-dependent one-to-one coordinate transformation,

$$\begin{aligned} \tau &= t \\ \zeta &= \zeta(t, y), \end{aligned} \tag{3}$$

is employed to map a physical domain with the moving boundary onto a unit interval. Note that the ζ coordinate depends on time and, therefore, a moving mesh technique is applied to solve the quasi-1-D Euler equations. Because the frequency of diaphragm oscillations ω is a given quantity, the moving mesh can be generated analytically

$$y(\zeta, \tau) = (1 - \zeta) \left[L + a(1 - \cos(\omega \tau)) \right], \tag{4}$$

where y and ζ are physical and computational coordinates, respectively, a and ω are the amplitude and frequency of diaphragm oscillation, and $L + a$ is a mean depth of the quasi-1-D synthetic jet actuator.

Diaphragm oscillations are forced by varying the position of the diaphragm $y(0, \tau)$ where the impermeable wall boundary condition is imposed. Because the deforming mesh Eq. (4) is given analytically, the diaphragm velocity can be calculated by differentiating Eq. (4) with respect to time to give

$$v(0, \tau) = a\omega \sin(\omega \tau). \tag{5}$$

It should be noted that the region near the jet exit requires special consideration. The full numerical simulation of the actuator orifice region is crucial for accurate prediction of the interaction between the synthetic jet and the external boundary layer. This region is characterized by strong flow separation that cannot be described by the quasi-1-D Euler equations. To overcome this problem, the quasi-1-D actuator model is used only to simulate the flow inside the actuator cavity, while the small region near the actuator orifice is modeled by solving the 2-D unsteady Navier-Stokes equations. This approach allows us to accurately predict the interaction of the synthetic jet with the external boundary layer and to resolve vortices generated in the vicinity of the actuator orifice, while reducing the computational cost.

The low-dimensional actuator model has several advantages. First, this approach is fully conservative and provides conservation of mass, momentum, and energy. Second, the new quasi-1-D model is computationally much more efficient compared with the 2-D or 3-D numerical simulation of the cavity flow. Third, the reduced-order model retains some important multidimensional features of the realistic actuator, such as the length, diaphragm deflection, and area variation. These properties of the new model and its ability to account for the compressibility effects inherent in actuator devices make it an efficient tool for quantitative study of the actuator resonance characteristics.

To demonstrate the ability of the new reduced-order model to quantitatively predict the 3-D actuator dynamics, the phase-averaged time history of vertical velocity over the center of the slot obtained with the quasi-1-D model and three different measurement techniques is shown in Fig. 2.

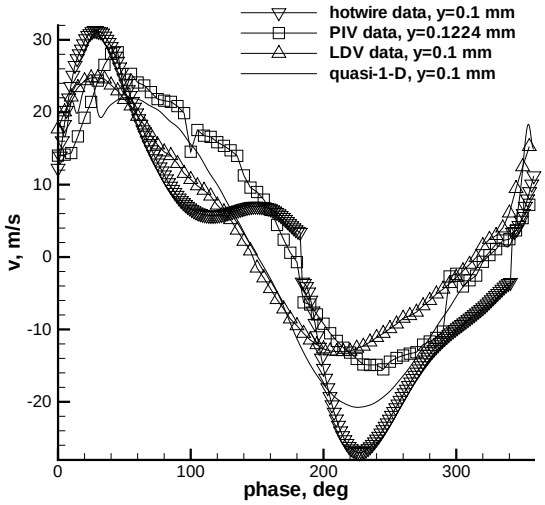

Figure 2: Phase-averaged time-history of the vertical velocity over the center of the slot, obtained with the quasi-1-D model and using the PIV, hotwire, and LDV measurement techniques.

Implementation and Case Specific Details

The simulations were started with quiescent flow and run through sufficient periods to obtain periodic solutions. This was usually about 10 periods. The experimentally determined diaphragm position was used to describe the moving boundary condition of the quasi-1-D actuator. The shape of the diaphragm was assumed to be the first mode of the Bessel function eigensolution of the cylindrical dram symmetric vibration. A scaling factor of 1.35 was later added to obtain the peak exit velocity that was in the Mach = 0.1 range.

Acknowledgments

The work of the first author was partially funded by NASA Langley Research Center and NIA.

References

[1] N.K. Yamaleev, M.H. Carpenter, A Reduced-Order Model for Efficient Simulation of Synthetic Jet Actuators, NASA/TM-2003-212664, December 2003, (submitted to AIAA Journal).

[2] M.H. Carpenter, D. Gottlieb, and S. Abarbanel, Time-Stable Boundary Conditions for Finite Difference Schemes Solving Hyperbolic Systems: Methodology and Application to High Order Compact Schemes, *Journal of Computational Physics*, Vol. 111, No. 2, April 1994.

[3] M.H. Carpenter, Jan Nordström, D. Gottlieb, A stable and Conservative Interface Treatment of Arbitrary Spatial Accuracy *Journal of Computational Physics*, Vol. 148, 341-365, (1999).

[4] J. Nordström, M.H. Carpenter, Boundary and Interface Conditions for High-Order Finite-Difference Methods Applied to the Euler and Navier-Stokes Equations *Journal of Computational Physics*, Vol. 148, 621-645, (1999).

[5] M.H. Carpenter, C.A. Kennedy, Fourth-Order 2N-Storage Runge-Kutta Schemes, NASA-TM-109112, April 1994.